HHS Public Access

Author manuscript

Biofactors. Author manuscript; available in PMC 2017 November 12.

Published in final edited form as:

Biofactors. 2016 November 12; 42(6): 703–715. doi:10.1002/biof.1304.

Pancreatic β-cell Production of CXCR3 Ligands Precedes Diabetes Onset

Susan J. Burke[1], **Michael D. Karlstad**[2], **Adrianna E. Eder**[2], **Kellie M. Regal**[2], **Danhong Lu**[3], **David H. Burk**[4], and **J. Jason Collier**[1]

[1]Laboratory of Islet Biology and Inflammation, Pennington Biomedical Research Center, Baton Rouge, LA

[2]Department of Surgery, Graduate School of Medicine, University of Tennessee Health Science Center, Knoxville, TN

[3]Sarah W. Stedman Nutrition and Metabolism Center, Duke Molecular Physiology Institute, Duke University School of Medicine, Durham, NC

[4]Cell Biology and Bioimaging Core Facility, Pennington Biomedical Research Center, Baton Rouge, LA

Abstract

Type 1 diabetes mellitus (T1DM) results from immune cell-mediated reductions in function and mass of the insulin-producing β-cells within the pancreatic islets. While the initial trigger(s) that initiates the autoimmune process is unknown, there is a leukocytic infiltration that precedes islet β-cell death and dysfunction. Herein, we demonstrate that genes encoding the chemokines CXCL9, 10, and 11 are primary response genes in pancreatic β-cells and are also elevated as part of the inflammatory response in mouse, rat, and human islets. We further established that STAT1 participates in the transcriptional control of these genes in response to the pro-inflammatory cytokines IL-1β and IFN-γ. STAT1 is phosphorylated within five minutes after β-cell exposure to IFN-γ, with subsequent occupancy at proximal and distal response elements within the Cxcl9 and Cxcl11 gene promoters. This increase in STAT1 binding is coupled to the rapid appearance of chemokine transcript. Moreover, circulating levels of chemokines that activate CXCR3 are elevated in non-obese diabetic (NOD) mice, consistent with clinical findings in human diabetes. We also report herein that mice with genetic deletion of CXCR3 (receptor for ligands CXCL9, 10, and 11) exhibit a delay in diabetes development after being injected with multiple low doses of streptozotocin. Therefore, we conclude that production of CXCL9, 10, and 11 from islet β-cells controls leukocyte migration and activity into pancreatic tissue, which ultimately influences islet β-cell mass and function.

Keywords

Autoimmunity; Chemokine; Diabetes; Inflammation; Islets; Transcription

Corresponding Author: J. Jason Collier, Ph.D., Laboratory of Islet Biology and Inflammation, Pennington Biomedical Research Center, 6400 Perkins Rd., Baton Rouge, LA 70808. Phone: (225) 763-2884; Fax: (225) 763-0274; Jason.collier@pbrc.edu.

The authors have no conflicts of interest to disclose.

Introduction

Reductions in function and/or mass of the pancreatic islet β-cells result in the clinical presentation of T1DM and T2DM (1, 2). Despite outwardly distinct etiologies, both T1DM and T2DM arise via inflammation-based events that alter pancreatic tissue function as well as the quantity of insulin-positive cells. The pro-inflammatory cytokines IL-1β and IFN-γ contribute to islet inflammation via transcriptional reprogramming events that include the production of chemokines (3–7). Chemokine receptors direct leukocyte migration to sites of inflammation and alter leukocytic activity via interactions with specific ligands (8). Ligand-mediated stimulation of individual chemokine receptors also controls precise aspects of immune cell action, including integrin expression and cytokine production (9). Thus, synthesis and release of chemokines by either islet β-cells, leukocytes, or both cell types contributes to T1DM, T2DM, rejection of transplanted islets, as well as other diseases with inflammatory components (10, 11, 6).

Development of T1DM is postulated to arise by selective autoimmune-mediated dysfunction and destruction of pancreatic islet β-cells (12, 13). This process has been studied extensively in non-obese diabetic (NOD) mice, a polygenic mouse model that spontaneously develops diabetes with many representative features of the human disease (14, 15). In addition, mice injected with multiple low doses of streptozotocin (MLDS) also develop diabetes associated with inflammatory activity and decreased islet β-cell mass. Both the NOD and MLDS mouse models display islet inflammation (16) and recruitment of T-lymphocytes into pancreatic tissue (17). Notably, one of major receptors responsible for directing migration of T-cell populations is CXCR3 (18).

CXCR3 is enriched on activated T cells, memory T cells and NK cells. $CD4^+$ and $CD8^+$ T-cells are responsive to the chemokine ligands CXCL9, CXCL10, and CXCL11 via the CXCR3 receptor (19, 18). In addition, CXCR3 ligands heighten T-cell receptor signaling during priming via activation of specific intracellular signaling events (20). Moreover, CXCR3 activation increases the production of IFN-γ, a cytokine that promotes macrophage activation, production of IL-1, islet inflammatory responses, and diabetes development (21, 22). Thus, the effects of pro-inflammatory cytokines (e.g., IL-1β, IFN-γ, etc.), coupled with CXCR3 activation by specific chemokine ligands, together may be responsible for a positive feedback mechanism ensuring repeated exposure of leukocytes, such as effector $CD8^+$ T cells, to specific antigens relevant for onset of T1DM. The long-term effect of chemokine-mediated priming, recruitment, and activation of leukocytic infiltrates appears to be destructive pro-inflammatory events within pancreatic islets.

IFN-γ, through the JAK-STAT pathway, participates in the regulated transcription of multiple genes controlling inflammation (23, 7). Moreover, IL-1β and IFN-γ synergize to induce the expression of specific genes in pancreatic β-cells, including those encoding the inducible nitric oxide synthase and the chemokine CXCL10 (24–26). The signal-specific phosphorylation of STAT1 by IFNs supports dimerization and enhanced transcriptional activity at precise genomic response elements (27). Our *in silico* analysis revealed enrichment in STAT1 binding sites within the promoters of the Cxcl9, Cxcl10, and Cxcl11

genes. While the molecular mechanisms underlying the transcriptional regulation of the Cxcl10 gene have been reported (25), the signaling events controlling expression of Cxcl9 and Cxcl11 chemokine-encoding genes in pancreatic β-cells have not been characterized. Therefore, in the present study, we report the molecular determinants required for signal-specific activation of genes encoding CXCR3 ligands and the impact of global genetic deletion of CXCR3 during diabetes induced by MLDS.

Experimental Procedures

Cell Culture, Islet Isolation and Reagents

The INS-1-derived rat insulinoma cells have been described previously (28, 29). These cell lines were cultured in RPMI-1640 (Sigma; St. Louis, MO) with 10% fetal bovine serum (FBS; Life Technologies Co., Carlsbad, CA). Seven week old female BALB/c (#000651) and 3, 7, and 8 week old NOD (#001976) mice were purchased from The Jackson Laboratory (Bar Harbor, ME) and allowed to acclimate to the photoperiod (12-hour light/12-hour dark) and temperature conditions (22 ± 1°C) of the animal facility for a minimum of one week. After acclimation, the mice were euthanized by CO_2 asphyxiation followed by cervical dislocation and pancreata were harvested for histological and immunohistochemical analyses. In a separate cohort of 10 week old male and 4, 8, and 12 week old female NOD (#001976) mice, islets were isolated as previously described (30). Rat islets were isolated according to previously published protocols (31). Human islets from three different donors were obtained through Lonza (Basel, Switzerland). IL-1β and IFN-γ was purchased from Peprotech (Rocky Hill, NJ). Cycloheximide was from Sigma. The JAK inhibitor was from EMD Millipore (Billerica, MA). Recombinant adenoviruses expressing β-galactosidase, 5xNF-κB-luciferase, and IκBα super-repressor have all been described (32). We have previously described the generation of recombinant adenoviruses expressing STAT1 mutants Y701F (33), S727A, S727T and the double mutant Y701F/S727A (25).

Diabetes induction by multiple low doses of streptozotocin (MLDS)

Eight week old CXCR3$^{-/-}$ (#005796) and CXCR3$^{+/+}$ (#000664; C57BL/6) mice were purchased from The Jackson Laboratory (Bar Harbor, ME) and allowed to acclimate to the animal facility for seven days prior to the beginning of the MLDS protocol. Mice were provided access to Harlan Teklad Laboratory Diet 8640 (Madison, WI) and water *ad libitum* throughout the study. Streptozotocin (S0130; STZ) was purchased from Sigma Aldrich (St. Louis, MO) and suspended in sterile sodium citrate buffer (0.1M, pH 4.5). At 9 weeks of age, the mice were weighed and randomly sorted into four groups: Vehicle CXCR3$^{-/-}$, Vehicle CXCR3$^{+/+}$, MLDS CXCR3$^{-/-}$, and MLDS CXCR3$^{+/+}$. During days 1–5, the treatment groups were administered a sterile intraperitoneal (i.p.) STZ injection (40 mg STZ / kg body weight). The vehicle control groups were administered an equal volume of sterile sodium citrate by i.p. injection every day for five consecutive days. Body weight and a tail vein blood sample were taken once a day during the injection period to measure blood glucose. Blood glucose was measured using the ACCU-CHEK Aviva PLUS Glucometer (Roche Diagnostics, Indianapolis, IN). During days 6–22, body weight was measured and a tail vein blood sample was taken twice a week to measure blood glucose. On day 23, mice were euthanized by CO_2 asphyxiation followed by cervical dislocation and pancreata were

harvested for histological and immunohistochemical analyses. Heart punctures were performed to obtain a final serum sample. In a separate study, 12 week old male C57BL/6J mice, obtained from The Jackson Laboratory, were given STZ by i.p. injection (40 mg / kg body weight) for five consecutive days followed by isolation of islets three and six days after the final injection. Our procedure for isolation of mouse islets has been described (30). Approximately one hundred islets from each mouse were used for RNA isolation. All protocols and procedures were approved by the University of Tennessee Institutional Care and Use Committees.

Pancreatic Islet Histology

After fixation in 10% neutral buffered formalin (NBF) for 24–48 hrs, pancreata were embedded in paraffin and 5 μm sections collected on positively charged slides. Immunohistochemical detection of insulin was performed on a Leica Bond-Max (Leica Biosystems, Melbourne, Australia) using the Bond Polymer Refine detection kit. Antibodies used were guinea pig anti-insulin (1:800, #18-0067, Invitrogen, Grand Island, NY) followed by 30 min with HRP-conjugated rabbit anti-guinea pig (1:800, A5545, Sigma, Saint Louis, MO). The anti-CD3 antibody was from Abcam (ab5690). Stained sections were imaged using a Hamamatsu NanoZoomer digital slide scanner at 20x resolution. For determination of insulin positive area, three-four mice per group were used and at least two sections from each mouse were cut, separated by ~200 μm. These sections were analyzed and quantified using a custom application within Visiopharm VIS software version 5.0.5.

Transfection of siRNA Duplexes

Silencer select siRNA duplexes (STAT1: s129043 and s129044 and silencer negative control no. 1: AM4611) from Life Technologies were transfected into 832/13 cells using DharmaFECT Transfection Reagent 1 (Thermo Scientific) according to the manufacturer's protocol.

RNA Isolation, cDNA synthesis and Real-time RT-PCR

Isolation of total RNA, cDNA synthesis and real-time RT-PCR have been previously described (34, 33). For all transcripts studied, the relative mRNA abundance was normalized to that of the housekeeping gene ribosomal S9. Approximately 100 islets per mouse were used for RNA isolation. Primers used in RT-PCR reactions were designed using Primer3Plus software and are available upon request.

Isolation of Protein and Immunoblot Analysis

Whole cell lysates were prepared using M-PER (Thermo Fisher Scientific) supplemented with protease and phosphatase inhibitor cocktails (Thermo Fisher Scientific). The protein concentration of the lysate was determined using the bicinchoninic acid (BCA) assay (Thermo Fisher Scientific) and immunoblotting was performed as previously described (25). Antibodies used for the detection of tubulin and total STAT1 were all from Cell Signaling.

ELISA

Serum levels of CXCL9, CXCL10, and CXCL11 were detected using the mouse CXCL9 Quantikine ELISA kit (Cat # MCX900), CXCL10 Quantikine ELISA kit (Cat # MCX100) and the mouse CXCL11 DuoSet ELISA kit (Cat # DY572), all from R&D Systems (Minneapolis, MN) using the protocol provided by the manufacturer. Serum levels of insulin were detected using the Ultrasensitive Mouse Insulin ELISA kit (Cat # 10-1249-01) from Mercodia (Uppsala, Sweden) according to their recommended procedures.

Chromatin Immunoprecipitation

Chromatin immunoprecipitation assays and data analysis were as previously described (25). Antibodies used for immunoprecipitation of STAT1 and PO_4-Y701 STAT1 were from Cell Signaling (Danvers, MA). Normal rabbit and mouse serum (IgG) were from Sigma. Primer sequences used to amplify genomic DNA were designed using Primer3Plus software and are available upon request.

Statistics

One-way ANOVA, followed by Tukey post-hoc correction, or Student *t* test was performed using GraphPad Prism 6 with corresponding *p* values indicated in the individual figure legends.

Results

The CXCR3 activating chemokines CXCL9, CXCL10, and CXCL11 are elevated in mouse, rat, and human islets during inflammation

The NOD mouse spontaneously develops diabetes with characteristics similar to the human disease (14, 15). Using islets isolated from 10 week old female NOD mice, we determined that expression of the Cxcl9, Cxcl10, and Cxcl11 genes are elevated 430, 10.9 and 4.3-fold, respectively, when compared to age-matched BALB/c controls (Figure 1A). We further note that islets from female NOD mice have elevated levels of chemokine gene expression relative to the age-matched male NOD mice (Figure 1A), consistent with the observations of accelerated immune cell influx into pancreatic tissue in the females of this model of T1DM (35). Next, we exposed isolated rat islets to IL-1β, IFN-γ, or a combination of these cytokines, and measured the expression of Cxcl9 and Cxcl11 genes. Cxcl9 is most responsive to IFN-γ, with a 376-fold increase in expression over control (untreated) islets (Figure 1B). Cxcl9 is largely unresponsive to IL-1β alone but its expression is synergistically enhanced when both IL-1β and IFN-γ are present (5908-fold; Figure 1B). The Cxcl11 gene was induced 46-fold by IL-1β, 8.7-fold by IFN-γ, and 215-fold in the presence of both cytokines (Figure 1C). The synergistic expression of the Cxcl9 and Cxcl11 genes by the combination of IL-1β and IFN-γ is consistent with the regulated expression of the Cxcl10 gene by these cytokines (25). This synergistic induction of genes encoding CXCR3 ligands is maintained when human islets are exposed to combinations of IL-1β and IFN-γ (Figure 1D–F).

Infiltration of T-lymphocytes into the pancreatic islets of NOD mice occurs prior to onset of hyperglycemia and is associated with enhanced levels of CXCL9 in serum

Blood glucose levels from female NOD mice at ages 4, 8, and 12 weeks were under 200 mg/dL and did not differ by age (Figure 2A). Similarly, body weights were not different between age matched (8 week old) BALB/c and NOD mice (Figure 2B). NOD mice gained weight with age as expected for healthy animals. Next, we measured $CD3^+$ cell infiltration into the pancreatic tissue. BALB/c mice were completely free of $CD3^+$ infiltrates (Figure 2C; far left panel), consistent with expectations for healthy islet tissue. While we note that a few islets from NOD mice at 4 weeks of age showed low to moderate $CD3^+$ immunoreactivity (9 $CD3^+$ islets/131 total islets; 7%), the majority of islets were free from lymphocytic invasion at this age (Figure 2C; panel second from left and data not shown). However, by 8 and 12 weeks of age, marked infiltration of $CD3^+$ cells was apparent in the female NOD pancreas (34% and 57% $CD3^+$, respectively), with many islets showing either peri-insulitis or were invasively infiltrated (Figure 2C; second from right and far right panels). By contrast, we observed no evidence of $CD3^+$ staining in C57BL/6J mice (not shown), consistent with our observations using BALB/c mice. Staining for CXCL9 in pancreatic islets indicated co-localization with the insulin-positive cells but not the leukocyte population (not shown). Using female NOD mice, we next measured serum levels of CXCL9 and CXCL10 at 4, 8, and 12 weeks of age. The increase in $CD3^+$ cell infiltration in female NOD mice is congruent with elevated levels of circulating CXCL9 and CXCL10 (compare with 10 week old male NOD mice; Figure 2D and 2E). Finally, we note that CXCL10 (Figure 2E) circulates at high levels early while CXCL9 follows the opposite pattern (Figure 2D) and both chemokines circulated in larger quantities in female NOD mice relative to male NOD mice. Serum levels of CXCL11 were undetectable in all strains of mice (data not shown).

The CXCL9, CXCL10, and CXCL11 genes are increased by pro-inflammatory cytokines and are primary response genes in β-cells

In 832/13 rat insulinoma cells, maximal expression of the Cxcl9, Cxcl10, and Cxcl11 genes occurred within 3–4 h (Figures 3A–C). IFN-γ robustly potentiated the IL-1β response for all three genes in 832/13 cells; comparable results were obtained using INS-1E rat insulinoma cells (not shown). Next, we investigated whether the cytokine-dependent induction of the Cxcl9, Cxcl10 and Cxcl11 genes required *de novo* protein synthesis (indicating secondary response genes) or whether these genes are truly primary response genes in β-cells. Cycloheximide completely blunted production of luciferase protein production driven by a 5xNF-κB promoter in response to IL-1β stimulation (data not shown), indicating the effectiveness of the chemical as a translational inhibitor to disrupt protein synthesis. By contrast, the cytokine-dependent expression of Cxcl9, Cxcl10, and Cxcl11 was largely unperturbed in the presence of cycloheximide (Figure 3 D–F). Because cytokine-mediated upregulation of these chemokine genes did not require *de novo* protein synthesis, we conclude that they are primary response genes in pancreatic β-cells exposed to these specific inflammatory stimuli.

JAK activation and STAT1 signaling are required for cytokine-mediated activation of genes encoding CXCR3 ligands

To determine how IFN-γ potently induces the Cxcl9 and Cxcl11 genes, we investigated the JAK-STAT pathway. We observed rapid phosphorylation of STAT1 (within 5 min) after exposure to IFN-γ (Figure 4A). We then used pharmacological inhibition of JAK1 and siRNA-mediated targeting of STAT1 to investigate signaling events relevant to transcription. Pharmacological inhibition of JAK1 reduced the ability of IFN-γ to potentiate the IL-1β–mediated induction of the Cxcl9 gene by 29 and 93% at 10 and 100 nM, respectively (Figure 4B). IFN-γ-mediated potentiation of the Cxcl11 gene was blunted by 49% with 100 nM JAK inhibitor (JAKi; Figure 4C). To directly examine STAT1 involvement, we used siRNA duplexes targeted against STAT1 mRNA. Using two different siRNA targeting sequences, we observed 86 and 88 % decreases in the IFN-γ mediated potentiation of the Cxcl9 gene (Figure 4D). Additionally, reductions in STAT1 abundance decreased the IFN-γ mediated potentiation of the Cxcl11 gene by 50 and 58% (Figure 4E). Cumulatively, these data indicate a requirement for the JAK1 and STAT1 proteins for maximal IFN-γ – stimulated expression of the Cxcl9 and Cxcl11 genes. These findings are also consistent with what has been reported previously for the Cxcl10 gene (25).

STAT1 phosphorylation at Y701, but not S727, is required for maximal cytokine-dependent activation of the Cxcl9 and Cxcl11 genes

Phosphorylation of STAT1 (Y701 and S727) is required for the expression of a variety of genes in many different cell types (36, 25, 26). To determine the importance of these sites for cytokine-mediated regulation of the Cxcl9 and Cxcl11 genes, we examined transcript abundance for Cxcl9 and Cxcl11 following adenoviral expression of either wild-type or phospho-mutant STAT1 proteins. Similar STAT1 protein levels were detected in response to overexpression of each recombinant wild-type and mutant STAT1 construct (Figure 5A). IFN-γ-mediated potentiation of the Cxcl9 gene is enhanced by STAT1 overexpression; this effect was not significantly diminished in the presence of the S727A or a more conservative S727T mutation within STAT1 (Fig. 5B). By contrast, removal of the tyrosine phosphoacceptor site at position 701 (Y701F) impairs the STAT1-dependent augmentation in response to IFN-γ (Figure 5B). The reduced expression of Cxcl9 observed with the STAT1 Y701F mutant is similar to the phenotype observed with the double mutation (DM; Y701F/S727A; Figure 5B).

In addition, overexpression of STAT1 also enhanced the IFN-γ-mediated potentiation of the Cxcl11 gene (2.6-fold to 4.2-fold; Figure 5C). Similar to results observed for Cxcl9, the Cxcl11 gene requires phosphorylation of STAT1 at Tyr701, but not Ser727, to support its expression in response to IFN-γ (Figure 5C). In isolated rat islets, the Y701F/ S727A mutant also decreased expression of the Cxcl9 (Figure 5D) and Cxcl11 (Figure 5E) genes by 84 and 61%, respectively. Taken together, the data in Figures 4 and 5 indicate that tyrosine phosphorylation of STAT1 supports cytokine-mediated induction of the Cxcl9 and Cxcl11 genes, which is congruent with regulation of the Cxcl10 gene (25).

Phosphorylated STAT1 is recruited to the Cxcl9 and Cxcl11 promoters in response to IFN-γ

Because of the requirement for STAT1 to support transcription of the Cxcl9, Cxcl10, and Cxcl11 genes in response to IFN-γ [see ref. (25) and Figures 4 and 5], we performed *in silico* analyses of the genomic response elements present upstream of the Cxcl9 and Cxcl11 coding regions to identify potential DNA sequences responsible for gene activation. Two putative IFN-γ-activated sequences (GAS) sites were identified in the promoters of each gene (see schematic). Therefore, we used chromatin immunoprecipitation assays to investigate the occupancy of STAT1 at each of these sites in response to IFN-γ. Proximal and distal GAS elements in the Cxcl9 (Figure 6A and B left panels) and Cxcl11 (Figure 6C and D left panels) promoters are indicated by the arrows in the schematic diagrams. STAT1 was detected at the Cxcl9 proximal (pGAS) and distal (dGAS) sites in the unstimulated state (value set at 1), with a clear increase in STAT1 ChIP signal in response to IFN-γ (Figures 6A and B middle panels). Similar results were seen on the Cxcl11 proximal (pGAS) and distal (dGAS) sites (Figures 6C and D middle panels).

We subsequently examined the occupancy of STAT1 phosphorylated at Tyr701 at the promoters of the Cxcl9 and Cxcl11 genes. We observed an increase in phosphorylated $STAT1^{Y701}$ occupancy at both the proximal (pGAS) and distal (dGAS) GAS elements in the Cxcl9 promoter at 5, 10, 15, 30 and 60 min stimulation with IFN-γ(Figure 6A and B right panels). Similar enhancements in $STAT1^{PO4\text{-}Y701}$ were detected at the proximal (pGAS) and distal (dGAS) GAS elements within the Cxcl11 promoter (Figure 6B and C right panels). These binding events are also congruent with the timing of STAT1 phosphorylation at Tyr701 (Figure 4A) and with appearance of transcript accumulation one hour after exposure to IFN-γ (Figure 3).

Genetic Deletion of CXCR3 Delays Onset of Hyperglycemia *in vivo*

CXCR3 ligands are produced in mouse, rat, and human islets in response to inflammatory signaling events [see Figures 1 and 3 in this study and refs (5, 25)]. Therefore, mice with genetic homozygous deletion of CXCR3 were monitored for onset of hyperglycemia after MLDS injection. Wild-type ($CXCR3^{+/+}$) mice developed elevated blood glucose levels (239 mg/dL) within 7 days after the last STZ injection (shown as day 12 in Figure 7A) while blood glucose levels for CXCR3 $^{-/-}$ mice averaged 191 mg/dL (Figure 7A). Eleven days after the last STZ injection, $CXCR3^{+/+}$ mice had blood glucose levels averaging 276 mg/dL compared with 230 mg/dL for $CXCR3^{-/-}$ mice (shown as day 16 in Figure 7A). Overall results showing percent of mice diabetic at glucose threshold levels of either 225 mg/dL or 250 mg/dL on two separate occasions are shown in Table 1. Circulating insulin levels at the end of the study were decreased in both STZ-injected groups (Figure 7B), consistent with the eventual onset of hyperglycemia in each group (Figure 7A). Pancreatic islet histology revealed a marked diminution in insulin positive cell area in both STZ-injected groups, consistent with a reduction in the pancreatic β-cell population (Figure 7C). Interestingly, there were 2.28-fold more insulin-positive cells in the $CXCR3^{-/-}$ mice treated with MLDS versus the $CXCR3^{+/+}$ mice at the end of the study period (Figure 7D; compared black bar to black bar). We further found that MLDS is associated with increased pancreatic islet expression of the Cxcl9 and Cxcl10 genes within three days after the final injection (Figures 7D and E), which is *prior to onset* of hyperglycemia. In addition, the islet expression levels

of Cxcl9, but not Cxcl10, remained elevated seven days after the final injection. This increase in islet expression of CXCR3 ligands is analogous to transcript elevations observed in NOD mice, which develop spontaneous autoimmune diabetes, and also consistent with isolated rat and human islets exposed to IL-1β and IFN-γ (Figure 1).

DISCUSSION

Islet β-cell destruction leading to T1DM is a leukocyte driven process with an unknown initial trigger (37). Experimentally, diabetes can be induced by multiple low doses of streptozotocin (MLDS), which generates sufficient islet β-cell damage to produce the onset of hyperglycemia. We show for the first time that the MLDS procedure induces the early expression of CXCR3 ligands within pancreatic islets (within 3 and 6 days; see Figures 7D and 7E). We therefore reasoned that if chemokine-mediated lymphocyte recruitment was directly responsible for alterations in islet β-cell mass and function, the production of ligands within pancreatic islets should occur prior to the onset of hyperglycemia.

Indeed, we found that islets isolated from both NOD mice and mice receiving MLDS displayed elevations in chemokine expression relevant to T-cell recruitment *prior to the development of overt hyperglycemia* (e.g., Cxcl9 and Cxcl10; see Figure 1A, Figure 7D, and Figure 7E). As a proof of principle in human tissues, higher levels of $CD8^+$ T cell infiltration into islets, that were also hyper-expressing MHC-I, were found in a male cadaveric donor positive for two autoantibodies (38). Importantly, this individual was not yet diabetic, which would fit our model of β-cell production of chemokines mediating the infiltration of immune cells into pancreatic tissue prior to diabetes onset.

In addition, clonal β-cell lines, as well as mouse, rat, and human islets exposed to IFN-γ or a combination of IL-1β and IFN-γ display increased expression of the genes encoding the CXCR3 ligands CXCL9, CXCL10, and CXCL11 (Figure 1 and Figure 3). Furthermore, part of the inflammatory response attributed to ageing includes increased expression of CXCL9 in pancreatic islets (39). We suspect that this elevated chemokine response in the pancreas occurs across species as an early signaling event to regulate immune cell activity within pancreatic tissue.

In the present study, we report that genetic deletion of CXCR3 slowed the onset, but did not prevent hyperglycemia induced by MLDS (Figure 7A). This *in vivo* result is consistent with the enhanced production of CXCR3 chemokines within pancreatic islets in response to inflammatory signals (Figures 1, 7D, and 7E). Collectively, the observations from isolated islets and the genetic deletion of CXCR3 are congruent with chemokine ligands engaging the cognate receptor (CXCR3) as part of the immunological process driving the onset of hyperglycemia. These results are also consistent with a reduction in diabetes in a viral model of islet β-cell destruction (40), showcasing a potential broad utility for CXCR3 inhibition to protect β-cells against inflammation-mediated events.

The reasons for incomplete protection against diabetes development upon CXCR3 deletion are not known at this time. However, redundancy in the chemokine system is at least a partial explanation for the phenotype shown herein as T-cells respond to many signals

beyond those activating the CXCR3 receptor. These include ligands activating the CCR4, CCR5, CCR6, and CCR7 receptors (41). Several of these chemokine receptors are linked to either autoimmune-mediated, obesity-associated, or both forms of diabetes (42–45, 30). In addition, combination therapies, such as anti-CD3 plus anti-CXCL10, are more effective at suppressing inflammatory responses that contribute to hyperglycemia than individual therapeutic interventions (46). Thus, targeting of more than one chemokine receptor or leukocyte subtype may be a better overall therapeutic strategy than selectively targeting a single receptor.

Enhanced activity of macrophages during the MLDS course of study could also contribute to a decline in insulin-positive cell mass via increased superoxide production (47). Activated macrophages produce and secrete IL-1β (48), a pro-inflammatory cytokine detrimental to islet β-cells (49, 6). Importantly, β-cell exposure to IL-1β decreases glucose-stimulated insulin secretion concomitant with elevations in chemokine synthesis and release (50). Moreover, NOD mice with NLRP3 deficiency have reduced incidence of hyperglycemia (51), at least in part due to decreased T-cell infiltration along with reduced IFN-γ production. Thus, decreased circulating insulin and increased chemokine production are two processes associated with diabetes development, indicating the importance of cytokine processing and signaling for autoimmune disease onset. Because CXCR3 is capable of activating macrophages in other experimental systems (52), it is possible that deletion of CXCR3 also reduces the resident macrophage contribution to islet inflammation, reducing the severity of MLDS-induced hyperglycemia.

Our results are consistent with those reported using mice deficient in the IFN-γ receptor, which display reduced $CD4^+$ T-cell-mediated destruction of islet β-cells (53). However, IFN-γ receptor deletion would be expected to provide a much broader basis for protection against the pathological consequences of inflammation when compared with targeting a single chemokine receptor (e.g., CXCR3). In our view, protection against diabetes by a reduction in signaling through the IFN-γ receptor would be due to decreased activation of many genes involved in inflammation, whereas CXCR3 deletion would ostensibly remove only the contribution from its cognate ligands (e.g., CXCL9, CXCL10, etc.).

On the other hand, enhanced islet expression of CXCL10 [an IFN-γ inducible, bona fide STAT1 target gene (25)] directly promotes leukocytic infiltration into pancreatic islets and subsequently contributes to acceleration of diabetes onset after viral infection (54). Collectively, the data presented herein are consistent with IFN-γ activation of STAT1 target genes in β-cells, which includes the synthesis and secretion of chemokines (e.g., CXCR3 ligands). The marked upregulation of chemokine production and secretion from β-cells enhances immune cell infiltration into pancreatic tissue, consistent with previous observations (55). The islet β-cell is therefore a source of chemoattractant molecules supporting leukocytic infiltration into the pancreas prior to the onset of hyperglycemia.

In summary, the data presented herein reflects rapid and robust production of chemokines capable of recruiting $CXCR3^+$ cells after islet β-cell exposure to pro-inflammatory stimuli. These events occur prior to onset of hyperglycemia in both NOD mice and C57BL/6J mice injected with MLDS. Deletion of CXCR3 affords only partial protection against

inflammation-mediated losses in islet β-cell mass. We interpret these data to indicate that targeting a single chemokine receptor, such as CXCR3, may be insufficient to fully prevent immune cell-mediated losses in islet β-cell mass and function. Further work is required to fully delineate the role of chemokine receptors, and associated primary response genes encoding chemokine receptor ligands, during leukocyte-mediated alterations in islet β-cell mass and function.

Acknowledgments

This work was supported partly by NIH grants P20-GM103528 (J.J.C.), 1 U54-GM104940 (J.J.C.), and R44-GM099207 (J.J.C. and M.D.K.).

This study was also supported in part by a grant from the Physicians' Medical Education and Research Foundation, Knoxville, TN (to J.J.C and M.D.K.).

This project used the PBRC Genomics and the Cell Biology and Bioimaging Core Facilities that are supported in part by COBRE (NIH8 P20-GM103528) and NORC (NIH 1P30-DK072476) center grants from the National Institutes of Health.

References

1. Meier JJ. Beta cell mass in diabetes: a realistic therapeutic target? Diabetologia. 2008; 51:703–713. [PubMed: 18317728]
2. Tuomi T, Santoro N, Caprio S, Cai M, Weng J, Groop L. The many faces of diabetes: a disease with increasing heterogeneity. Lancet. 2014; 383:1084–1094. [PubMed: 24315621]
3. von Herrath MG, Oldstone MB. Interferon-gamma is essential for destruction of beta cells and development of insulin-dependent diabetes mellitus. J Exp Med. 1997; 185:531–539. [PubMed: 9053453]
4. Arnush M, Heitmeier MR, Scarim AL, Marino MH, Manning PT, Corbett JA. IL-1 produced and released endogenously within human islets inhibits beta cell function. J Clin Invest. 1998; 102:516–526. [PubMed: 9691088]
5. Sarkar SA, Lee CE, Victorino F, Nguyen TT, Walters JA, Burrack A, Eberlein J, Hildemann SK, Homann D. Expression and regulation of chemokines in murine and human type 1 diabetes. Diabetes. 2012; 61:436–446. [PubMed: 22210319]
6. Burke SJ, Collier JJ. Insulitis and Diabetes: A Perspective on Islet Inflammation. Immunome Research. 2014; 10 Special Issue: Cytokine Biology.
7. Burke SJ, Collier JJ. Transcriptional Regulation of Chemokine Genes: A Link to Pancreatic Islet Inflammation? Biomolecules. 2015; 5:1020–1034. [PubMed: 26018641]
8. Baggiolini M. Chemokines and leukocyte traffic. Nature. 1998; 392:565–568. [PubMed: 9560152]
9. Karin N, Wildbaum G, Thelen M. Biased signaling pathways via CXCR3 control the development and function of CD4+ T cell subsets. J Leukoc Biol. 2015
10. Gerard C, Rollins BJ. Chemokines and disease. Nat Immunol. 2001; 2:108–115. [PubMed: 11175802]
11. Merani S, Truong WW, Hancock W, Anderson CC, Shapiro AM. Chemokines and their receptors in islet allograft rejection and as targets for tolerance induction. Cell Transplant. 2006; 15:295–309. [PubMed: 16898223]
12. Castano L, Eisenbarth GS. Type-I diabetes: a chronic autoimmune disease of human, mouse, and rat. Annu Rev Immunol. 1990; 8:647–679. [PubMed: 2188676]
13. Laron Z, Hampe CS, Shulman LM. The urgent need to prevent type 1 autoimmune childhood diabetes. Pediatric endocrinology reviews : PER. 2015; 12:266–282. [PubMed: 25962204]
14. Driver JP, Chen YG, Mathews CE. Comparative genetics: synergizing human and NOD mouse studies for identifying genetic causation of type 1 diabetes. Rev Diabet Stud. 2012; 9:169–187. [PubMed: 23804259]

15. Jayasimhan A, Mansour KP, Slattery RM. Advances in our understanding of the pathophysiology of Type 1 diabetes: lessons from the NOD mouse. Clin Sci (Lond). 2014; 126:1–18. [PubMed: 24020444]
16. Anderson MS, Bluestone JA. The NOD mouse: a model of immune dysregulation. Annu Rev Immunol. 2005; 23:447–485. [PubMed: 15771578]
17. Herold KC, Montag AG, Fitch FW. Treatment with anti-T-lymphocyte antibodies prevents induction of insulitis in mice given multiple doses of streptozocin. Diabetes. 1987; 36:796–801. [PubMed: 3556279]
18. Groom JR, Luster AD. CXCR3 in T cell function. Exp Cell Res. 2011; 317:620–631. [PubMed: 21376175]
19. Groom JR, Luster AD. CXCR3 ligands: redundant, collaborative and antagonistic functions. Immunol Cell Biol. 2011; 89:207–215. [PubMed: 21221121]
20. Newton P, O'Boyle G, Jenkins Y, Ali S, Kirby JA. T cell extravasation: demonstration of synergy between activation of CXCR3 and the T cell receptor. Mol Immunol. 2009; 47:485–492. [PubMed: 19767105]
21. Boraschi D, Censini S, Tagliabue A. Interferon-gamma reduces macrophage-suppressive activity by inhibiting prostaglandin E2 release and inducing interleukin 1 production. J Immunol. 1984; 133:764–768. [PubMed: 6330202]
22. Sarvetnick N, Shizuru J, Liggitt D, Martin L, McIntyre B, Gregory A, Parslow T, Stewart T. Loss of pancreatic islet tolerance induced by beta-cell expression of interferon-gamma. Nature. 1990; 346:844–847. [PubMed: 2118234]
23. Stark GR, Darnell JE Jr. The JAK-STAT pathway at twenty. Immunity. 2012; 36:503–514. [PubMed: 22520844]
24. Heitmeier MR, Scarim AL, Corbett JA. Interferon-gamma increases the sensitivity of islets of Langerhans for inducible nitric-oxide synthase expression induced by interleukin 1. J Biol Chem. 1997; 272:13697–13704. [PubMed: 9153221]
25. Burke SJ, Goff MR, Lu D, Proud D, Karlstad MD, Collier JJ. Synergistic Expression of the CXCL10 Gene in Response to IL-1beta and IFN-gamma Involves NF-kappaB, Phosphorylation of STAT1 at Tyr701, and Acetylation of Histones H3 and H4. J Immunol. 2013; 191:323–336. [PubMed: 23740952]
26. Burke SJ, Updegraff BL, Bellich RM, Goff MR, Lu D, Minkin SC Jr, Karlstad MD, Collier JJ. Regulation of iNOS Gene Transcription by IL-1beta and IFN-gamma Requires a Coactivator Exchange Mechanism. Mol Endocrinol. 2013; 27:1724–1742. [PubMed: 24014650]
27. Levy DE, Darnell JE Jr. Stats: transcriptional control and biological impact. Nat Rev Mol Cell Biol. 2002; 3:651–662. [PubMed: 12209125]
28. Asfari M, Janjic D, Meda P, Li G, Halban PA, Wollheim CB. Establishment of 2-mercaptoethanol-dependent differentiated insulin-secreting cell lines. Endocrinology. 1992; 130:167–178. [PubMed: 1370150]
29. Hohmeier HE, Mulder H, Chen G, Henkel-Rieger R, Prentki M, Newgard CB. Isolation of INS-1-derived cell lines with robust ATP-sensitive K+ channel-dependent and -independent glucose-stimulated insulin secretion. Diabetes. 2000; 49:424–430. [PubMed: 10868964]
30. Burke SJ, Karlstad MD, Regal KM, Sparer TE, Lu D, Elks CM, Grant RW, Stephens JM, Burk DH, Collier JJ. CCL20 is elevated during obesity and differentially regulated by NF-kappaB subunits in pancreatic beta-cells. Biochim Biophys Acta. 2015; 1849:637–652. [PubMed: 25882704]
31. Collier JJ, Fueger PT, Hohmeier HE, Newgard CB. Pro- and antiapoptotic proteins regulate apoptosis but do not protect against cytokine-mediated cytotoxicity in rat islets and beta-cell lines. Diabetes. 2006; 55:1398–1406. [PubMed: 16644697]
32. Collier JJ, Burke SJ, Eisenhauer ME, Lu D, Sapp RC, Frydman CJ, Campagna SR. Pancreatic beta-Cell Death in Response to Pro-Inflammatory Cytokines Is Distinct from Genuine Apoptosis. PLoS One. 2011; 6:e22485. [PubMed: 21829464]
33. Burke SJ, Collier JJ. The gene encoding cyclooxygenase-2 is regulated by IL-1beta and prostaglandins in 832/13 rat insulinoma cells. Cell Immunol. 2011; 271:379–384. [PubMed: 21885043]

34. Burke SJ, Collier JJ, Scott DK. cAMP prevents glucose-mediated modifications of histone H3 and recruitment of the RNA polymerase II holoenzyme to the L-PK gene promoter. J Mol Biol. 2009; 392:578–588. [PubMed: 19631660]
35. Young EF, Hess PR, Arnold LW, Tisch R, Frelinger JA. Islet lymphocyte subsets in male and female NOD mice are qualitatively similar but quantitatively distinct. Autoimmunity. 2009; 42:678–691. [PubMed: 19886740]
36. Wen Z, Zhong Z, Darnell JE Jr. Maximal activation of transcription by Stat1 and Stat3 requires both tyrosine and serine phosphorylation. Cell. 1995; 82:241–250. [PubMed: 7543024]
37. Atkinson MA, Eisenbarth GS, Michels AW. Type 1 diabetes. Lancet. 2014; 383:69–82. [PubMed: 23890997]
38. Rodriguez-Calvo T, Suwandi JS, Amirian N, Zapardiel-Gonzalo J, Anquetil F, Sabouri S, von Herrath MG. Heterogeneity and Lobularity of Pancreatic Pathology in Type 1 Diabetes during the Prediabetic Phase. J Histochem Cytochem. 2015; 63:626–636. [PubMed: 26216138]
39. Sandovici I, Hammerle CM, Cooper WN, Smith NH, Tarry-Adkins JL, Dunmore BJ, Bauer J, Andrews SR, Yeo GS, Ozanne SE, Constancia M. Ageing is associated with molecular signatures of inflammation and type 2 diabetes in rat pancreatic islets. Diabetologia. 2016; 59:502–511. [PubMed: 26699651]
40. Frigerio S, Junt T, Lu B, Gerard C, Zumsteg U, Hollander GA, Piali L. Beta cells are responsible for CXCR3-mediated T-cell infiltration in insulitis. Nat Med. 2002; 8:1414–1420. [PubMed: 12415259]
41. Islam SA, Luster AD. T cell homing to epithelial barriers in allergic disease. Nat Med. 2012; 18:705–715. [PubMed: 22561834]
42. Kim SH, Cleary MM, Fox HS, Chantry D, Sarvetnick N. CCR4-bearing T cells participate in autoimmune diabetes. J Clin Invest. 2002; 110:1675–1686. [PubMed: 12464673]
43. Carvalho-Pinto C, Garcia MI, Gomez L, Ballesteros A, Zaballos A, Flores JM, Mellado M, Rodriguez-Frade JM, Balomenos D, Martinez AC. Leukocyte attraction through the CCR5 receptor controls progress from insulitis to diabetes in non-obese diabetic mice. Eur J Immunol. 2004; 34:548–557. [PubMed: 14768060]
44. Yamazaki T, Yang XO, Chung Y, Fukunaga A, Nurieva R, Pappu B, Martin-Orozco N, Kang HS, Ma L, Panopoulos AD, Craig S, Watowich SS, Jetten AM, Tian Q, Dong C. CCR6 regulates the migration of inflammatory and regulatory T cells. J Immunol. 2008; 181:8391–8401. [PubMed: 19050256]
45. Shan Z, Xu B, Mikulowska-Mennis A, Michie SA. CCR7 directs the recruitment of T cells into inflamed pancreatic islets of nonobese diabetic (NOD) mice. Immunol Res. 2014; 58:351–357. [PubMed: 24687731]
46. Lasch S, Muller P, Bayer M, Pfeilschifter JM, Luster AD, Hintermann E, Christen U. Anti-CD3/anti-CXCL10 antibody combination therapy induces a persistent remission of type 1 diabetes in two mouse models. Diabetes. 2015
47. Kantwerk-Funke G, Burkart V, Kolb H. Low dose streptozotocin causes stimulation of the immune system and of anti-islet cytotoxicity in mice. Clin Exp Immunol. 1991; 86:266–270. [PubMed: 1657463]
48. Nathan CF. Secretory products of macrophages. J Clin Invest. 1987; 79:319–326. [PubMed: 3543052]
49. Corbett JA, Kwon G, Turk J, McDaniel ML. IL-1 beta induces the coexpression of both nitric oxide synthase and cyclooxygenase by islets of Langerhans: activation of cyclooxygenase by nitric oxide. Biochemistry. 1993; 32:13767–13770. [PubMed: 7505613]
50. Burke SJ, Stadler K, Lu D, Gleason E, Han A, Donohoe DR, Rogers RC, Hermann GE, Karlstad MD, Collier JJ. IL-1beta reciprocally regulates chemokine and insulin secretion in pancreatic beta-cells via NF-kappaB. Am J Physiol Endocrinol Metab. 2015; 309:E715–726. [PubMed: 26306596]
51. Hu C, Ding H, Li Y, Pearson JA, Zhang X, Flavell RA, Wong FS, Wen L. NLRP3 deficiency protects from type 1 diabetes through the regulation of chemotaxis into the pancreatic islets. Proc Natl Acad Sci U S A. 2015; 112:11318–11323. [PubMed: 26305961]
52. Zhou J, Tang PC, Qin L, Gayed PM, Li W, Skokos EA, Kyriakides TR, Pober JS, Tellides G. CXCR3-dependent accumulation and activation of perivascular macrophages is necessary for

homeostatic arterial remodeling to hemodynamic stresses. J Exp Med. 2010; 207:1951–1966. [PubMed: 20733031]

53. Yi Z, Li L, Garland A, He Q, Wang H, Katz JD, Tisch R, Wang B. IFN-gamma receptor deficiency prevents diabetes induction by diabetogenic CD4+, but not CD8+, T cells. Eur J Immunol. 2012; 42:2010–2018. [PubMed: 22865049]
54. Rhode A, Pauza ME, Barral AM, Rodrigo E, Oldstone MB, von Herrath MG, Christen U. Islet-specific expression of CXCL10 causes spontaneous islet infiltration and accelerates diabetes development. J Immunol. 2005; 175:3516–3524. [PubMed: 16148094]
55. Roep BO, Kleijwegt FS, van Halteren AG, Bonato V, Boggi U, Vendrame F, Marchetti P, Dotta F. Islet inflammation and CXCL10 in recent-onset type 1 diabetes. Clin Exp Immunol. 2010; 159:338–343. [PubMed: 20059481]

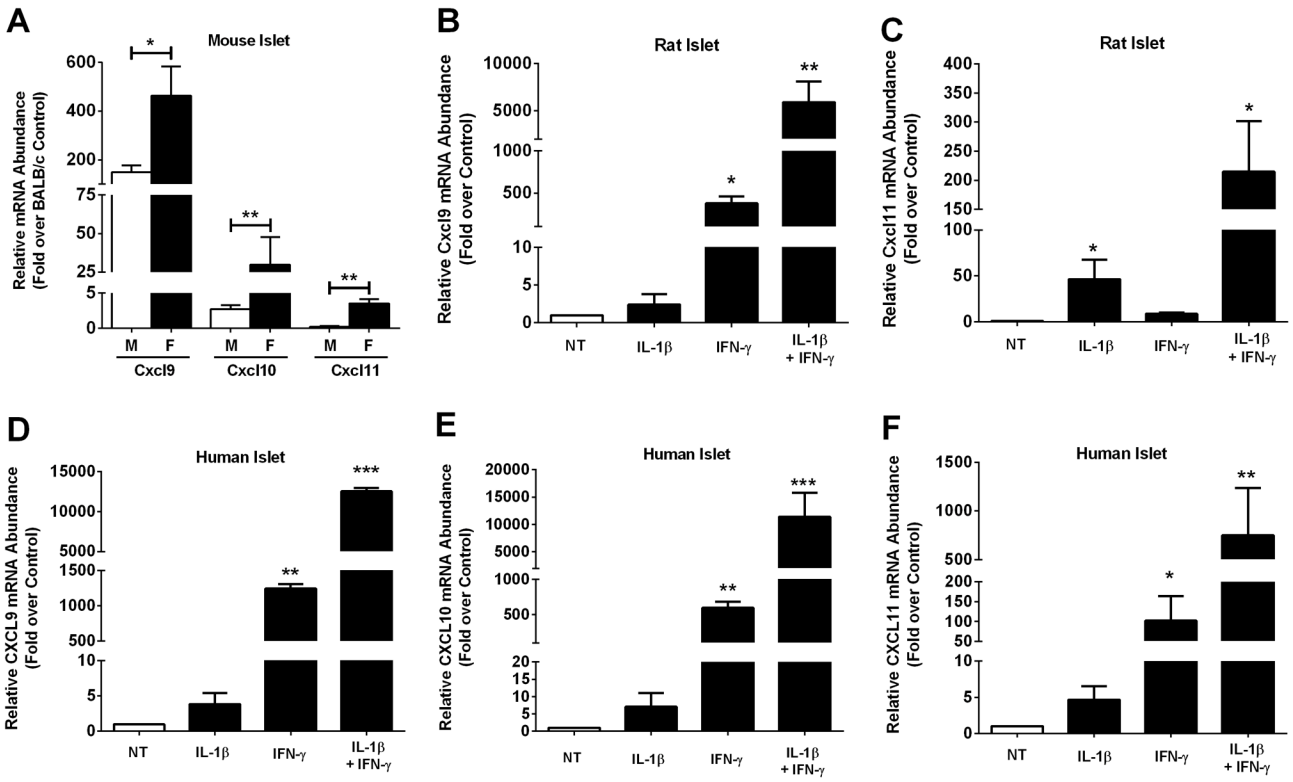

Figure 1. The CXCR3 activating chemokines CXCL9, CXCL10, and CXCL11 are elevated in mouse, rat, and human islets during inflammation

A. Cxcl9, Cxcl10 and Cxcl11 transcript levels were measured in islets isolated from 10 week old male (n = 4) and female NOD mice (n = 5). Data are expressed relative to age-matched BALB/c control mice (n = 7). $^{**}p<0.01$, $^{*}p<0.05$. **B–F**. Islets from Wistar rats (**B, C**; n = 4 per group) or human islets (**D–F;** n =3 per group) were untreated (NT) or stimulated with 10 ng/mL IL-1β, 100 U/mL IFN-γ or both cytokines for 3 h. **B–F**. Relative mRNA abundance of CXCL9 (**B, D**), CXCL10 (**E**) and CXCL11 (**C, F**) was determined by RT-PCR. $^{***}p<0.001$ vs. NT, $^{**}p<0.01$ vs. NT, $^{*}p<0.05$ vs. NT.

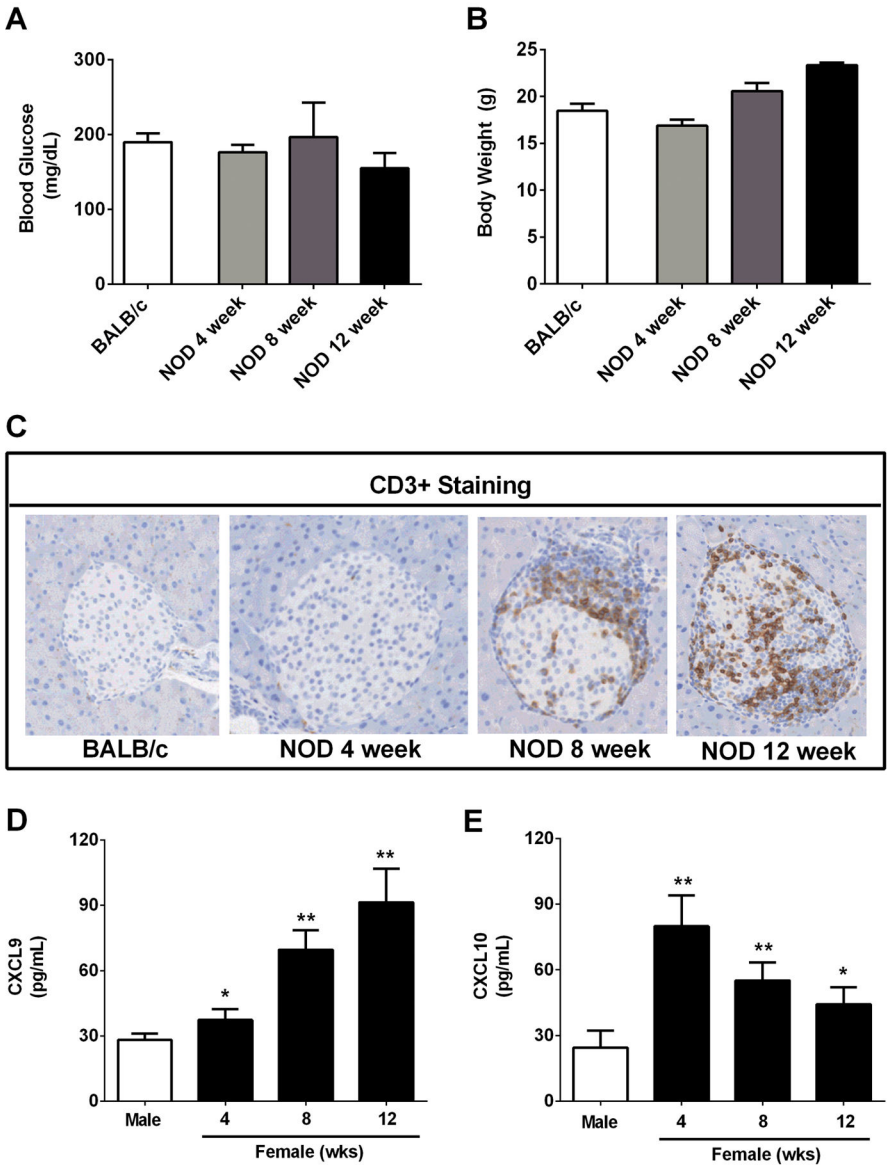

Figure 2. Infiltration of T-lymphocytes into the pancreatic islets of NOD mice occurs prior to onset of hyperglycemia but is consistent with enhanced levels of CXCL9 and CXCL10 in serum

A–C. Blood glucose (**A**), body weight (**B**) and $CD3^+$ staining (**C**) were assessed in 8 week old female BALB/c and 4, 8, and 12 week old female NOD mice. D,**E**. Serum CXCL9 **(D)** and CXCL10 **(E)** levels were determined in both male and female NOD mice (n = 4 mice per group). $^{**}p<0.01$ vs. male, $^{*}p<0.05$ vs. male.

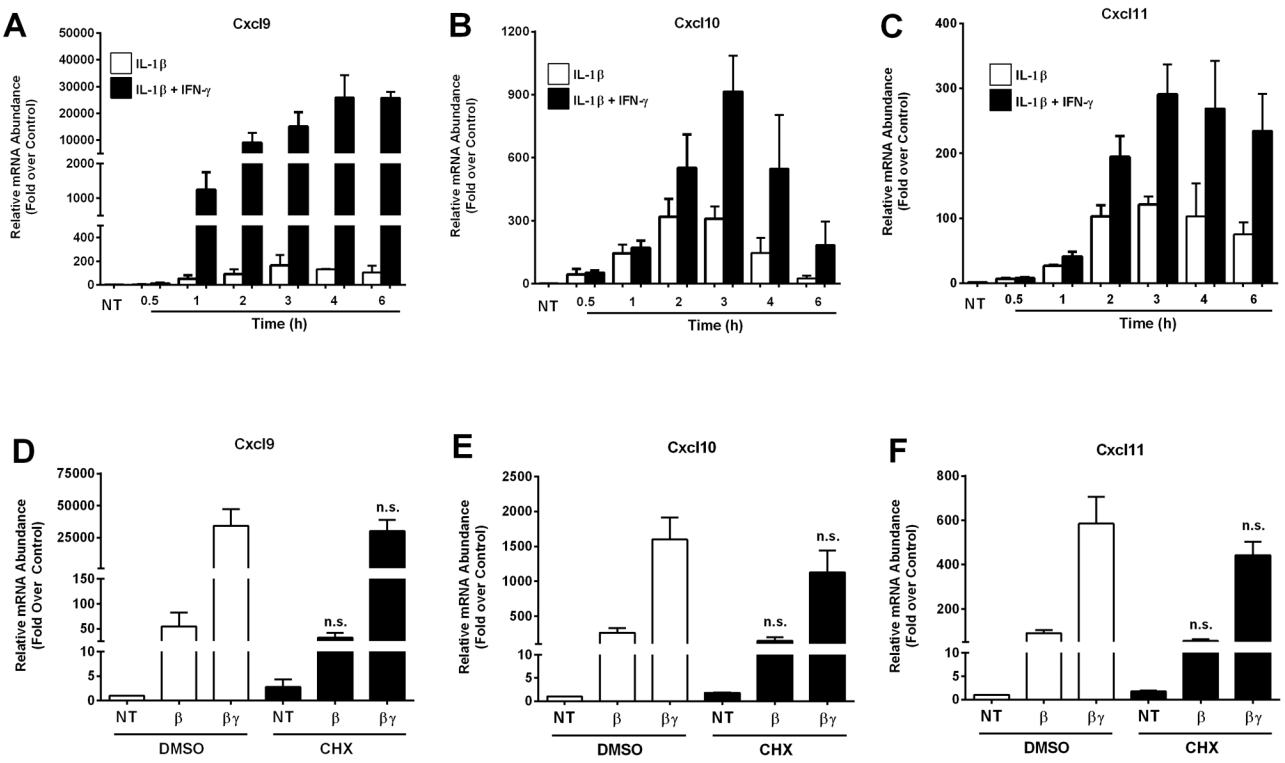

Figure 3. Expression of the Cxcl9, Cxcl10 and Cxcl11 genes is increased in a cytokine-dependent manner in rat β-cell lines

A–C. 832/13 rat insulinoma cells were stimulated with 1 ng/mL IL-1β or IL-1β plus 100 U/mL IFN-γ for the indicated times (NT; no treatment). **D–F**. 832/13 cells were pretreated for 1 h with either DMSO or 0.5 μg/mL Cycloheximide (CHX). Cells were subsequently exposed to IL-1β (1 ng/mL) or the combination of IL-1β and IFN-γ (100 U/mL) for 2 h. Cellular mRNA levels of Cxcl9 (**A, D**), Cxcl10 (**B, E**) and Cxcl11 (**C, F**) were detected by RT-PCR. n.s. = not significant vs respective treatment in DMSO control group. Data are shown as means ± SEM from three independent experiments.

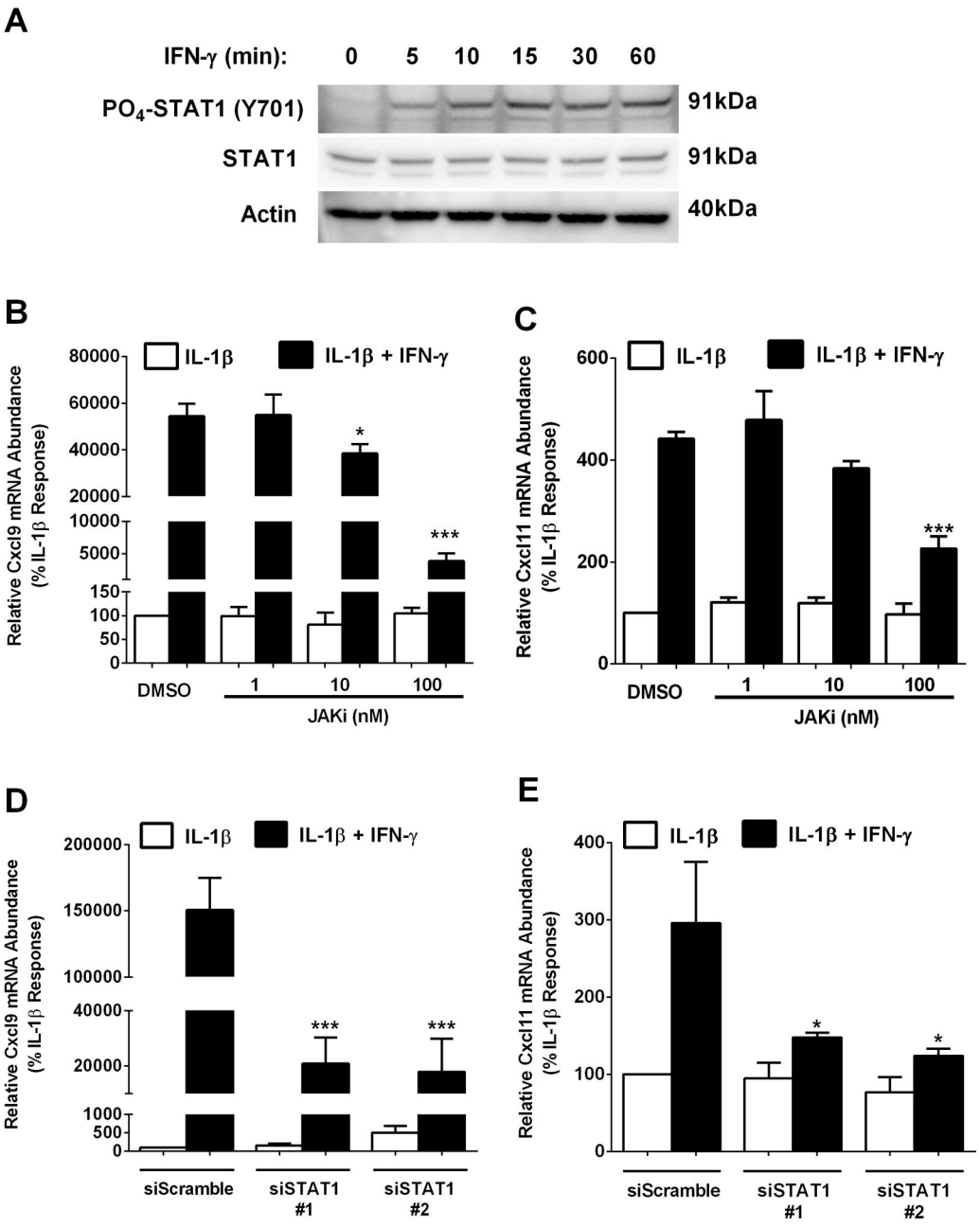

Figure 4. The JAK- STAT1 signaling pathway is required for cytokine-mediated activation of the Cxcl9 and Cxcl11 genes

A. 832/13 cells were exposed to 100 U/mL IFN-γ for the indicated times. PO_4-$STAT1^{Y701}$ and total STAT1 protein abundance were determined by immunoblotting. **B, C**. 832/13 cells were pre-treated for 1 h with increasing concentrations of JAKi (1 nM, 10 nM, 100 nM), followed by a 3 h stimulation with IL-1β alone (1 ng/mL) or IL-1β plus 100 U/mL IFN-γ. ***p<0.001 vs. DMSO (black bar), *p<0.05 vs. DMSO (black bar). **D, E**. 832/13 cells were transfected with two siRNA duplexes targeting STAT1 using a scrambled siRNA sequence duplex as a control. 48 h post- transfection cells were cultured for 3 h with 1 ng/ml IL-1β or IL-1β plus 100 U/ml IFN-γ. ***p<0.001 vs. siScramble (black bar), *p<0.05 vs. siScramble

(black bar). Cxcl9 (**B, D**) and Cxcl11 (**C, E**) mRNA levels were quantified. Data are represented as means ± SEM from three independent experiments. The immunoblot in A was repeated on two separate occasions.

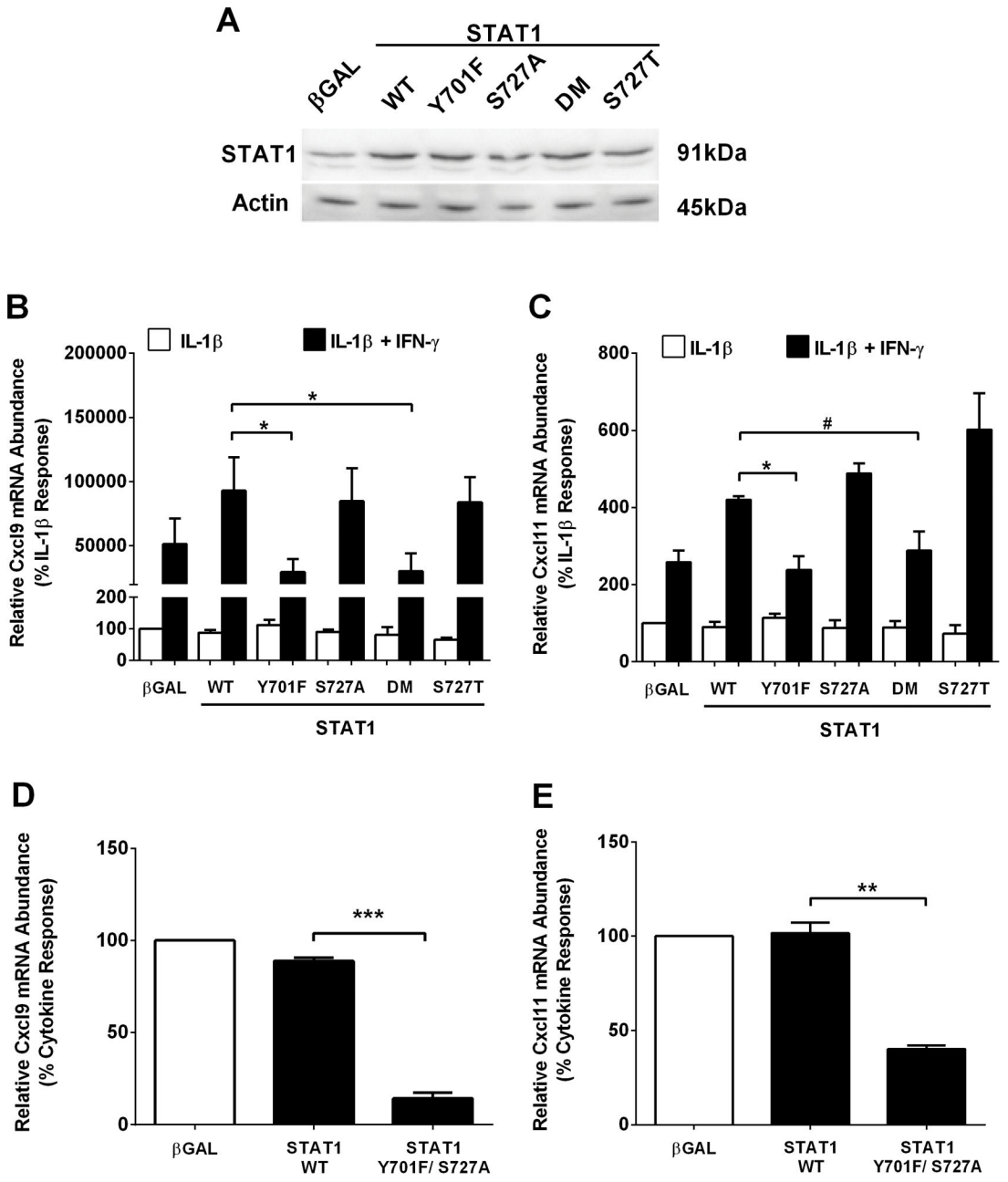

Figure 5. STAT1 phosphorylation at Y701, but not S727, is required for maximal cytokine-dependent activation of the Cxcl9 and Cxcl11 genes

A. 832/13 cells were transduced with adenoviruses encoding either βGAL, wild-type STAT1 (WT), $STAT1^{Y701F}$, $STAT1^{S727A}$, $STAT1^{Y701F/S727A}$ (DM; double mutant) or $STAT1^{S727T}$. STAT1 abundance was determined by immunoblotting. **B, C**. 832/13 cells were transduced with the adenoviruses indicated in (**A**); 24 h post-transduction cells were stimulated for 3 h with either IL-1β (1 ng/mL) alone or IL-1β plus IFN-γ (100 U/mL). $*p<0.05$, $^{\#}p<0.1$. **D, E**. Rat islets were transduced with the indicated adenoviruses. 24 h post-transduction cells were stimulated with both IL-1β (10 ng/mL) and IFN-γ (100 U/mL) for 3 h. $***p<0.001$, $**p<0.01$. Relative mRNA abundance of Cxcl9 (**B, D**) and Cxcl11 (**C, E**) was determined by

RT-PCR. Date are expressed as means ± SEM from 3 (**B, C**) or 2 (**D, E**) individual experiments. The immunoblot in A was repeated on two individual occasions.

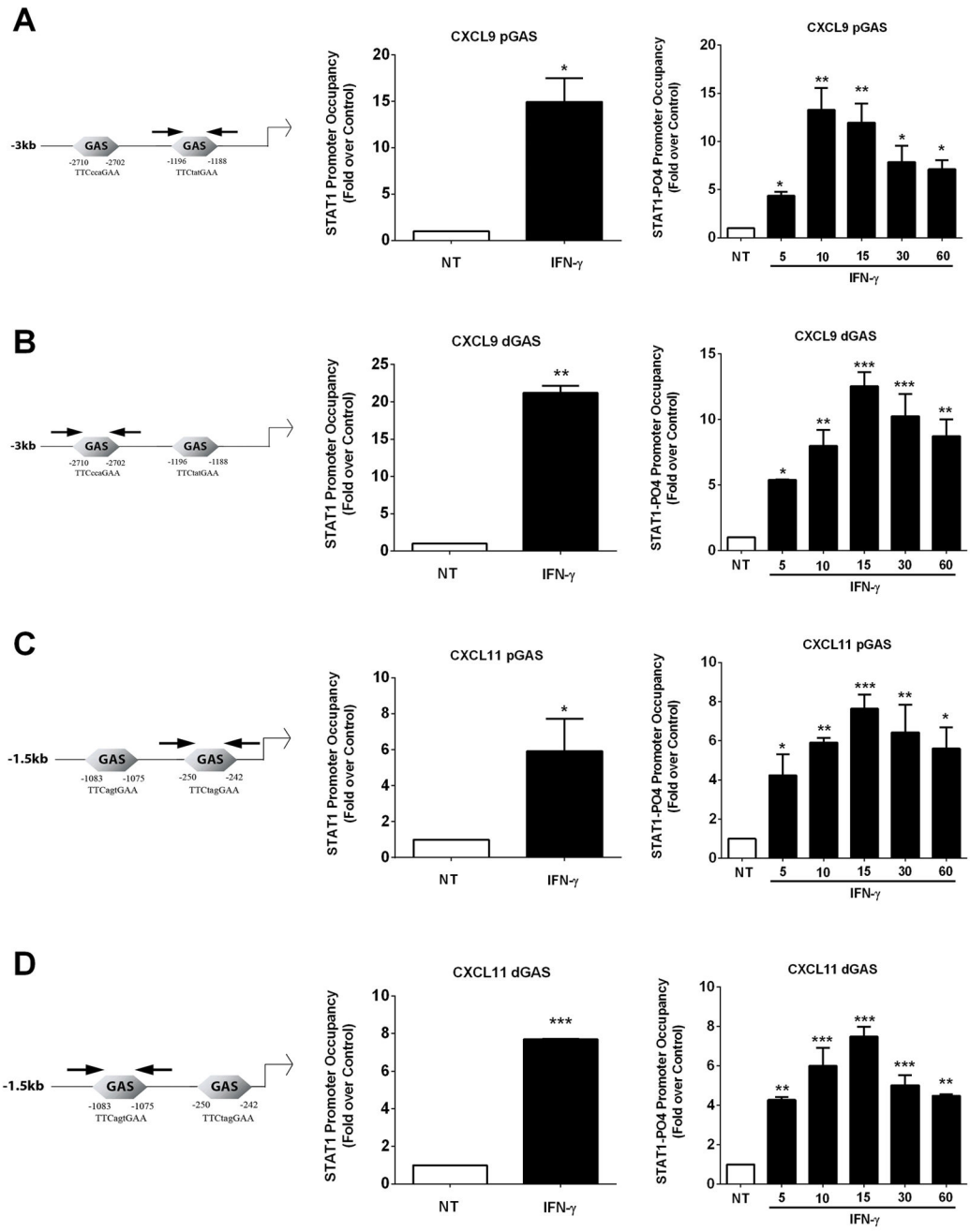

Figure 6. Phosphorylated STAT1 is recruited to the Cxcl9 and Cxcl11 promoters in response to IFN-γ

Schematic representation of distal and proximal GAS sites in the Cxcl9 and Cxcl11 promoters are shown (*left panels*). Arrows are the diagrammatic depiction of PCR amplicons. **A–D**. 832/13 cells were stimulated with 100 U/mL IFN-γ for either 20 mins (*middle panels*) or a time course (*right panels*). ChIP assays were performed to determine relative occupancy of total STAT1 (*middle panels*) and PO_4-$STAT1^{Y701}$ (*right panels*) on the Cxcl9 proximal (**A**) and distal promoter (**B**), and on the Cxcl11 proximal (**C**) and distal (**D**)

promoter. ***p<0.001 vs. NT, **p<0.01 vs. NT, *p<0.05 vs. NT. Data are expressed as means ± SEM from 3–4 individual experiments.

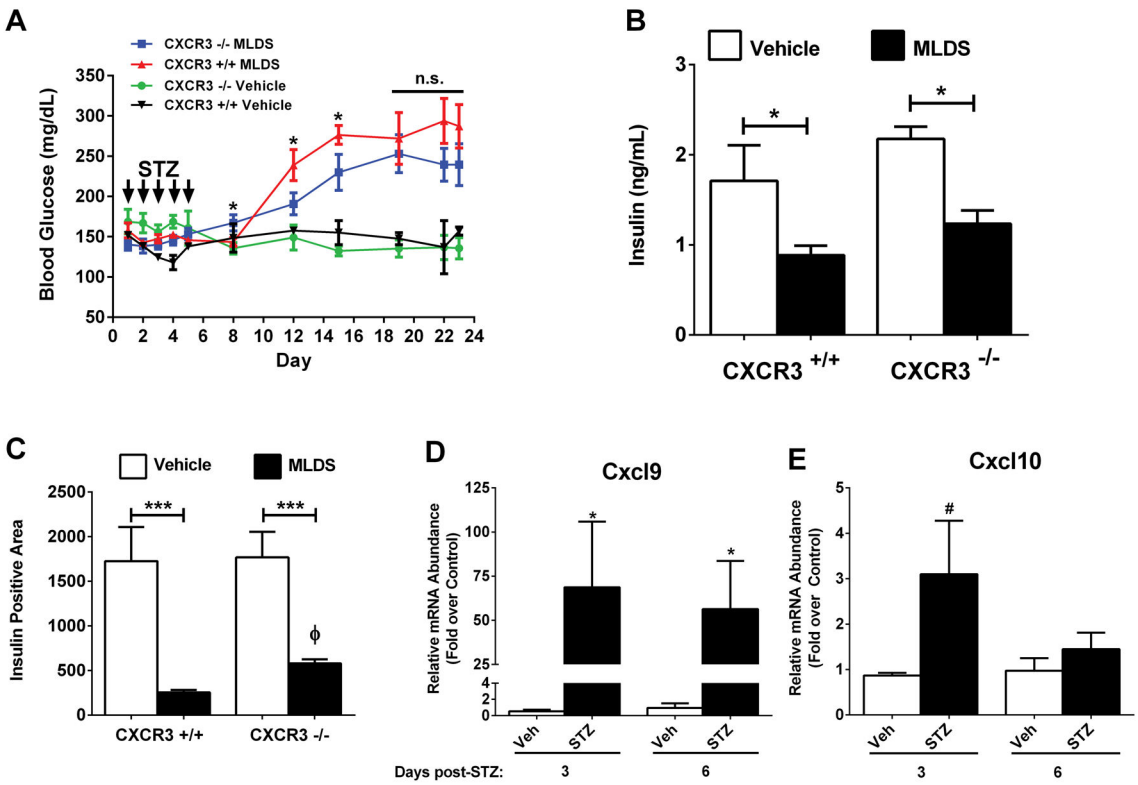

Figure 7. Genetic Deletion of CXCR3 Delays Onset of Hyperglycemia Induced by Multiple Low Doses of Streptozotocin

A. Blood glucose levels in control (CXCR3$^{+/+}$) and CXCR3 knockout (CXCR3$^{-/-}$) mice were monitored for 23 days after starting the MLDS protocol (n = 9 per group). *p<0.05 vs. CXCR3$^{-/-}$ on respective days. **B**. Serum insulin levels were measured 23 days after initiation of MLDS protocol. **C**. Insulin positive area from formalin-fixed, paraffin-embedded pancreatic tissue was quantified (n = 9 per group). **D, E**. C57BL/6J mice were injected with STZ for 5 consecutive days. Islets were isolated at 3 and 6 days following the last injection, and transcript levels of Cxcl9 (**D**) and Cxcl10 (**E**) were determined by qPCR. ***p<0.001 **(C)**, *p<0.05 **(D)**, $^{\#}p$<0.1 **(E)**, Φ, p<0.05 vs. CXCR3$^{+/+}$ **(C)**.

Table 1

Threshold	>225mg/dL		>250mg/dL	
	CXCR3+/+	**CXCR3−/−**	**CXCR3+/+**	**CXCR3−/−**
Frequency (%)	9/9 (100%)	6/9 (67%)	5/9 (56%)	3/9 (33%)